# Faraday Discussions

Accepted Manuscript


This manuscript will be presented and discussed at a forthcoming Faraday Discussion meeting. All delegates can contribute to the discussion which will be included in the final volume.

**Register now to attend!** Full details of all upcoming meetings: http://rsc.li/fd-upcoming-meetings

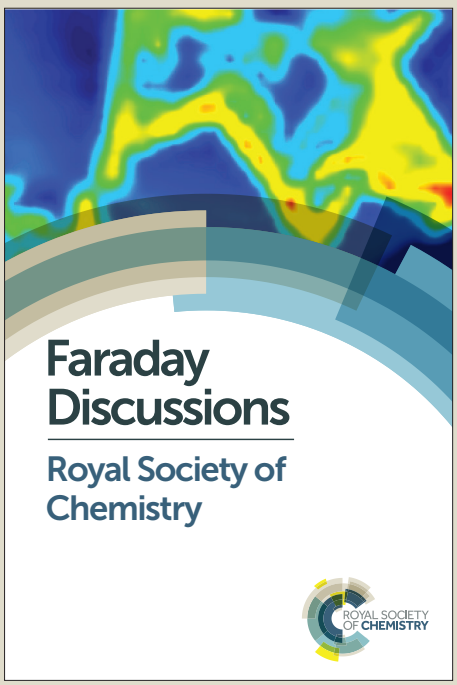


This is an *Accepted Manuscript*, which has been through the Royal Society of Chemistry peer review process and has been accepted for publication.

*Accepted Manuscripts* are published online shortly after acceptance, before technical editing, formatting and proof reading. Using this free service, authors can make their results available to the community, in citable form, before we publish the edited article. We will replace this *Accepted Manuscript* with the edited and formatted *Advance Article* as soon as it is available.

You can find more information about *Accepted Manuscripts* in the Information for Authors.

Please note that technical editing may introduce minor changes to the text and/or graphics, which may alter content. The journal's standard Terms & Conditions and the Ethical guidelines still apply. In no event shall the Royal Society of Chemistry be held responsible for any errors or omissions in this *Accepted Manuscript* or any consequences arising from the use of any information it contains.

ROYAL SOCIETY OF CHEMISTRY

www.rsc.org/faraday_d

Journal Name

RSCPublishing

ARTICLE

# Spinning of carbon nanotube fibres using the floating catalyst high temperature route: purity issues and the critical role of sulphur

Cite this: DOI: 10.1039/x0xx00000x

Received ooth January 2012,
Accepted ooth January 2012

DOI: 10.1039/x0xx00000x

www.rsc.org/

T. S. Gspann [a], F. R. Smail [a], A. H. Windle* [a]

The CVD process for the spinning of carbon nanotube (CNT) fibres [1] combines the nucleation, growth and aggregation of CNTs in the form of an aerogel with fibre spinning into a single process step. Optimisation of the process requires agility in multi-dimensional parameter space, so one tends to find parameter 'islands' where spinning is possible while exploration tends to follow 'routes' through this space. Here, we follow two such routes, one of which drastically improves fibre purity, the other changes the nature of the nanotubes comprising the fibres from multiwall to single wall. In the first case there is only a modest enhancement of mechanical properties, but in the second a very considerable improvement is seen. In terms of the conditions required to make fibres comprising predominately single wall CNTs, the key appears to be the rigorous control of sulphur addition, in trace quantities, coupled with the availability of carbon atoms at the earliest stage after injection, typically in the range 400 – 500°C. A model is presented for the role of sulphur in floating catalysts CNT synthesis.

## Introduction

Direct-spun carbon nanotube (CNT) fibres show values of tensile strength and stiffness [2,3] which are competitive with other high performance fibres such as traditional carbon fibre and Kevlar, while their yarn-like character endows them with a much higher knot efficiency [4], meaning that they can be knotted or woven with little, if any loss of tensile strength. The central challenge, however, remains. We are unable to transfer a sensible fraction of the vastly superior mechanical performance of individual CNTs [5,6] into a macroscopic structural material, even when the nanoubes are aligned axially as in a fibre. The fibre structure itself is hierarchical comprising of aligned bundles of CNTs, where each bundle consists of well aligned individual nanotubes [1,7]. The bundles are networked by nanotube exchange. The other two major methods for CNT fibre production such as liquid-crystal spinning [8,9] or spinning from forests [10,11] each generate very clean structures, as the CNTs are grown first and, at least in case of liquid-crystal spinning, can be cleaned very effectively prior to the spinning. However, these processes consist of at least 2, if not more steps. Additionally, the CNTs can be shortened as a result of any cleaning or purification stages. The attraction of the direct CNT fibre spinning process, first published by Ya-Li Li et al. [1], lies in the fact that it consists of one single process step, with extraction of an aligned aerogel of long nanotubes from a floating catalyst CVD system leading directly to the final yarn, which is wound up continuously. However, co-synthesised impurities and catalyst residues have been a problem for a long time. We present here methods for greatly reducing the impurity content of the fibre, and show how, through critical control of sulphur content, fibre can be grown which comprises of only single wall nanotubes. In the latter case a model is presented for the role of sulphur in floating catalyst synthesis.

## Experimental

### Spinning under standard conditions: particulate defects

The observation that fibres were stronger if tested at short gauge lengths, coupled with the observation of particulate defects, led [3] to surmise that property improvement would come simply from purity improvement. In part, this approach is one motivation for this current study. Here we refer to 'standard conditions' as those employed over much of our research on

direct spun CNT fibres over the past 5 years or more. Reactor conditions are set as described in Table 1.

*Table 1: Standard spinning conditions in a reactor tube with inner diameter 85 mm, reactor hot zone at 1290°C*

| Flow rates | | | | Overall atomic ratio | |
|---|---|---|---|---|---|
| $H_2$ [l/min] | Methane [ml/min] | Ferrocene [mg/min] | Thiophene [mg/min] | S:C | S:Fe |
| 0.8 | 80 | 0.35 | 1.3 | 0.004 | 7.65 |

Kumar [12] has summarised the different types of defects which can occur within the internal microstructure of CNT fibres. Of these, we focus on extraneous material largely in particulate form, which can be classified as: iron catalyst residue which has not given rise to nanotubes, or particles consisting of carbonaceous material which appears to be a secondary growth of extremely highly deformed multiwalled CNTs which entangle together forming larger clusters several micrometres in diameter (Figure 1a).

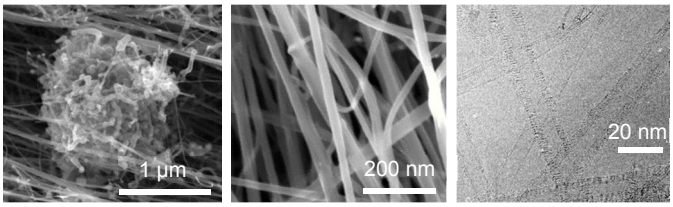


*Figure 1: (a) SEM of large impurity cluster composed of poorly formed MWCNTs and (b) well formed CNT bundles in a region remote from any particles. (c) TEM of nanotubes of the order of 10 nm in diameter, showing double and few walled examples.*

**What we know about the direct spinning process**

The direct spinning process has at its heart high temperature, floating catalyst, nanotube synthesis as a continuous flow (Figure 2). A centrally important advantage of spinning at 1290°C with added sulphur rather than 650 - 800°C without sulphur, is that the nanotubes do not deposit on the reactor walls in the reaction zone. One reason, to be discussed below, is that the sulphur prevents the iron deposited on the reactor wall from nucleating and growing nanotubes. Another reason why this does not occur, certainly in the main hot zone of the reactor, is thermophoresis or the so-called 'Ludwig-Soret' effect; namely that within a mean free path of the hot reactor wall, gas molecules are leaving a little faster than they arrive, so any nano-scale particle within that distance of the wall will experience a repulsion away from the wall.

In the direct-spinning process, the CNTs grow tangentially on the catalyst particles, so the size of catalyst particles is one of the most crucial factors controlling the type of CNTs grown. The size of the catalyst particles is mainly defined by two temperatures, namely the breakdown temperature of ferrocene and the temperature of the thermocatalytic breakdown of the carbon source on the catalyst surface. Due to the temperature profile, the difference between these two temperatures corresponds to a certain vertical distance in the reactor tube and, for a given flow velocity profile, a particular journey time.

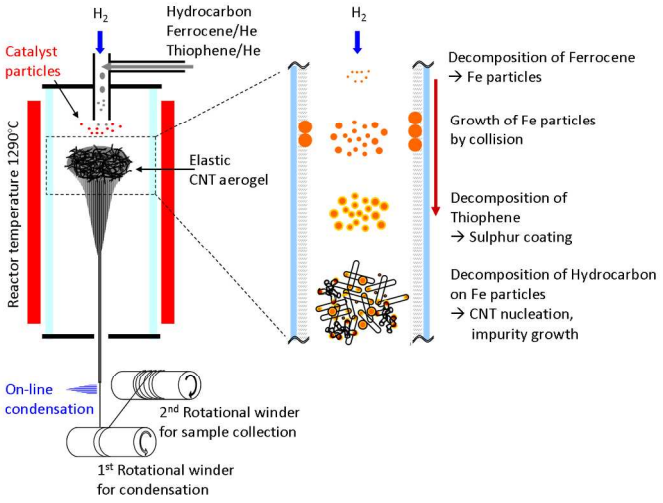


*Figure 2: Overview schematic of the CVD process for the direct spinning of CNT fibres and detailed schematic of the decomposition of the precursors leading to the formation of an elastic CNT aerogel.*

The modelled flow and heat transfer characteristics [13, 14] indicated that there was very little temperature gradient across the reactor tube; and for the flow rates normally employed, the flow was laminar being an order of magnitude or more below the critical Reynolds number, so a Poiseuille velocity distribution was established within 1.5 tube diameters below the injector (little or no jetting). These papers also demonstrated that once the catalyst particles had grown by collision, to the point where their Brownian diffusion rate in the plane normal to the reactor axis became large compared with mean gas flow rate, the particles could be considered entrained in a particular region of the transverse velocity profile. Hence those particles nearer the outside wall will be moving much slower, and thus have a longer residence time, and more opportunity for growth by collision before the temperature cross section is reached where nanotube growth commences. Figure 3a is adapted from Conroy et al. It emphasises that particle entrainment, and thus faster motion close to the reactor tube axis, becomes more significant with increasing particle size as the Brownian radial diffusion rates decrease. As the particles nearer to the walls travel more slowly, they will be bigger at any given cross section. The assumption also behind these calculations of iron particle coarsening is that particle contact definitely means coalescence, although it has been argued [15] that coalescence may be less rapid on account of sulphur on the particles.

There is another hydrodynamic effect which is possibly of significance. Segre and Silberberg [16,17] first showed experimentally that particles entrained within Poiseuille flow, after a certain distance from the entrance point into the reactor, would segregate into an annular region, close to the walls of the circular tube (typically at 0.63 times the radius). Their data are summarised in Figure 3b. For smaller particles the segregation within the central half of the tube is not as pronounced, although the outer 10% of the radius remains essentially

particle free. As their experiments were carried out with particles in the 0.1 – 1 mm range, larger by several orders of magnitude than our iron particles, we would not expect them to be relevant to the reaction described here. However, the concentration of nanotubes into an annular region is often observed in our reactor (we call the effect a 'sock' (SOM1)), so, with Conroy et al., we are reluctant to dismiss the relevance of this segregation effect as established by fluid dynamicists.

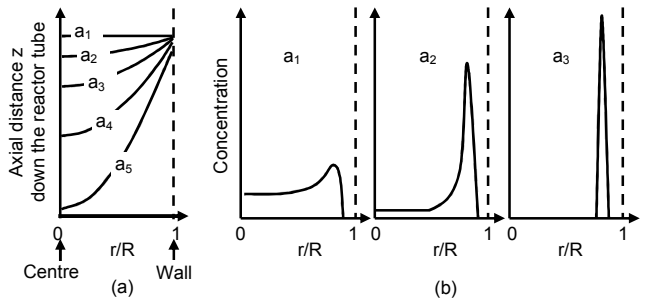


*Figure 3: (a) Distributions of catalyst particle diameters $a_i$ in a parabolic flow profile (a1 < a2 < an) in a reactor tube with diameter 2R (adapted from [13]). For a given distance down the reactor, a cross section through the particle diameter contours gives the lateral particle size distribution with considerable larger sizes nearer to the reactor walls. The actual particle sizes, given in the Conroy paper are not included here, as the conditions for which they were calculated, especially a ferrocene decomposition temperature of 1000°C, are not appropriate to the experimental conditions we explore here. (b) Derived concentration distribution of rigid particles of neutral density in a Poiseuille flow profile for a1 < a2 < a3 (adapted from [16]). The bigger the particles the more distinct is the formation of an annular ring. However, these experiments were executed for particle sizes several orders higher than described here.*

**Availability of components from precursors.** The literature would suggest that ferrocene begins to thermally decompose to liberate iron at around 500°C [18,19], but as soon as Fe is available it catalyses the decomposition of further ferrocene (autocatalysis) [20,14]. We have evidence of iron deposit on the reactor tube at the point of reactant injection at 400°C and thus believe that iron becomes available immediately on injection, whether through the action of this surface deposit or by the Brownian back diffusion of iron nuclei from hotter regions against the flow, is not yet clear.

There is extensive literature on the decomposition of thiophene catalysed by transition metals, although none specific to iron. In all the cases reported the metal surface will cause the breaking of the carbon sulphur bonds at temperatures even as low as room temperature, while the remaining hydrocarbon fragments are broken down at temperatures below 400°C. [21,22,23] The process is utilised to remove sulphur from natural hydrocarbons with the preferred catalyst being molybdenum. We conclude that in the presence of iron both as particles or present on the internal surfaces of the reactor, the thiophene will certainly be decomposed at the injection temperature of 400°C. Hence sulphur is available once iron has been liberated from the ferrocene. Furthermore, sulphur has long been understood as a growth accelerator [24,25] for carbon filaments on Fe particles, and we find it necessary to grow carbon nanotubes sufficiently quickly to form the coherent aerogel mandatory for the spinning process.

It should also be noted that the carbon component of the decomposition of both ferrocene and thiophene is not insignificant, and may be available for reconstruction on the surface of the growing iron particles. In this context we note a report that it is possible to synthesise carbon nanotubes from ferrocene alone [18], albeit in an argon atmosphere rather than hydrogen, noting that for ferrocene 10 carbon atoms are supplied for each iron atom. However, while the early carbon from the remains of the thiophene and ferrocene molecule may enable nanotube nucleation, their growth to a length at which they will entangle, and thus form the aerogel capable of being spun into the fibre, will depend on the availability of carbon from the decomposition of the main carbon precursor.

The initial experiments described here depend on methane as the major source of carbon. Methane is known as the most stable hydrocarbon and thermocatalytic breakdown on the Fe particle surface will not even start below temperatures of 680°C [26,27,28]. Toluene, which is used as the main carbon source in the final experiment described below, breaks down at a lower temperature, indeed it is routinely used as the carbon source in nanotubes synthesis at temperatures as low as 600°C where the metal catalyst is based on a substrate [29].

**Conversions Efficiencies.** The percentage of carbon converted into fibre is typically of the order of ~2% for the 'standard conditions' spinning. The lost carbon will consist of carbonaceous particles and nanotubes not incorporated into the fibre and removed from the reactor at the gas valve. There is also residual methane in the gas removed showing that not all the hydrocarbon has reacted [30]. It should be added that the laboratory rig has not been optimised for efficiency of conversion. Perhaps more startling is the fraction of iron, added as ferrocene, which is actually used in growing nanotubes. It is comparatively straightforward to determine the fraction of the iron incorporated within the nanotubes, as iron, or its oxide, after its quantitative analysis by TGA in air. For standard conditions (Figure 5a) there is some 10% by weight of iron (as opposed to 15% oxide recorded by the TGA) as catalyst residue within the fibre. For a ferrocene injection rate of 0.34 mg/min (0.10 mg/min Fe), we find that more than half of the iron injected as ferrocene can be accounted for in the fibre produced (SOM2). Making the reasonable assumption that decomposition of the ferrocene is complete after traversing the hot zone at 1290°C, then the non-incorporated iron has either been removed by the gas valve in particulate form, or plated onto the inside of the reactor tube. Indeed iron deposits are seen on the inside of the reactor tube starting level with the injector and then continuing until the temperature of the tube reaches ~1000°C where it becomes too sparse to detect. It is interesting to note that in the region of 700 – 800°C there is a thin deposit of carbon on top of the iron. The deposit of iron on the inside of the tube underlines the fact that the reactor tube, while not being the substrate for nanotube growth as occurs in lower temperature nanotube synthesis where there is no sulphur in the feedstock, is nevertheless a factor in determining the exact reactor conditions.

However, with much of the iron being incorporated within the fibres, it is instructive to determine the fraction which is actually involved in the nucleation and growth of the long nanotubes comprising the fibre. If we assume that our nanotubes are at least 100 µm long – and we have made an estimate in the past of an upper limit of 1 mm, despite it being a rather difficult experiment to conduct [3], further that they are on average triple wall and 10 nm in outside diameter [7], then an estimate of the fractional weight of iron (Fe/(Fe+C)) to catalyse such a tube would be $\sim 5 \cdot 10^{-4}$. It thus appears that, for an iron content in the fibre of 10%, 99.5% of the iron by mass is not used in the actual generation of nanotubes, but is incorporated within the nanotube fibre as much larger particles often covered with carbon typically as very poorly formed short multiwall CNTs. However, any attempt to significantly reduce the proportion of iron injected causes the process, - in terms of producing a dense 'cloud' of nanotubes with sufficient mechanical integrity to be spun-, to stop working. It thus appears that the nucleation of a nanotube from an iron particle is a chancy affair, with a very low success rate, so it is necessary to have a huge excess of particles available.

An important aspect of the process can be described as 'mechanical fractionation', in that one could expect that only those nanotubes long enough to entangle to give a mechanically coherent aerogel will be capable of being wound out of the reactor and drawn into a fibre. Once the nanotubes qualify, by virtue of spatial density and length, to form an aerogel, they are removed from the reactor mechanically at a rate typically 20 times the mean velocity of the gas flow. However, the presence of a significant particulate content within the fibre, based largely on the excess and redundant iron present, means that this ideal of mechanical fractionation is not being achieved. Process development to improve the purity of the fibre will now be described.

**Improvement in Purity**

We observed that if we increased the flow rate of the hydrogen gas, then the particle content of the fibres decreased. However, as these experiments approached the design limitation of the equipment, we achieved faster flow through the alternative approach of reducing the reactor tube diameter from 85 to 65 mm while maintaining the same volumetric gas flow rate, so in this case the ratio of hydrogen to reactants was maintained constant. This comparatively modest increase in the velocity through the reactor led to a dramatic reduction in entrapped particles. This approach also had the additional advantage that, as the volumetric rate was maintained, we did not have to adjust the wind-up rate, which otherwise would have implications for nanotube orientation within the fibre.

SEM images of the standard conditions material already described above (Figure 4a–d) show a high amount of co-synthesised impurity clusters which can be observed on the outside, while focussed ion beam (FIB) milled cross-sections and longitudinal sections show significant voids associated with embedded impurities. However, the sample spun in the smaller diameter reactor tube (Figure 4e–h), i.e. with a steeper velocity profile, show a dramatically cleaner and denser structure, not disrupted by any big impurities.

Thermogravimetric analysis (TGA) supports the observation of enhanced cleanliness by particle fractionation. The standard conditions material (Figure 5a), containing a high level of particle impurities showed typically two combustion events which could be identified as an impurity burning event at ~560°C and a clean bundles burning event approximately 100°C higher (SOM3).

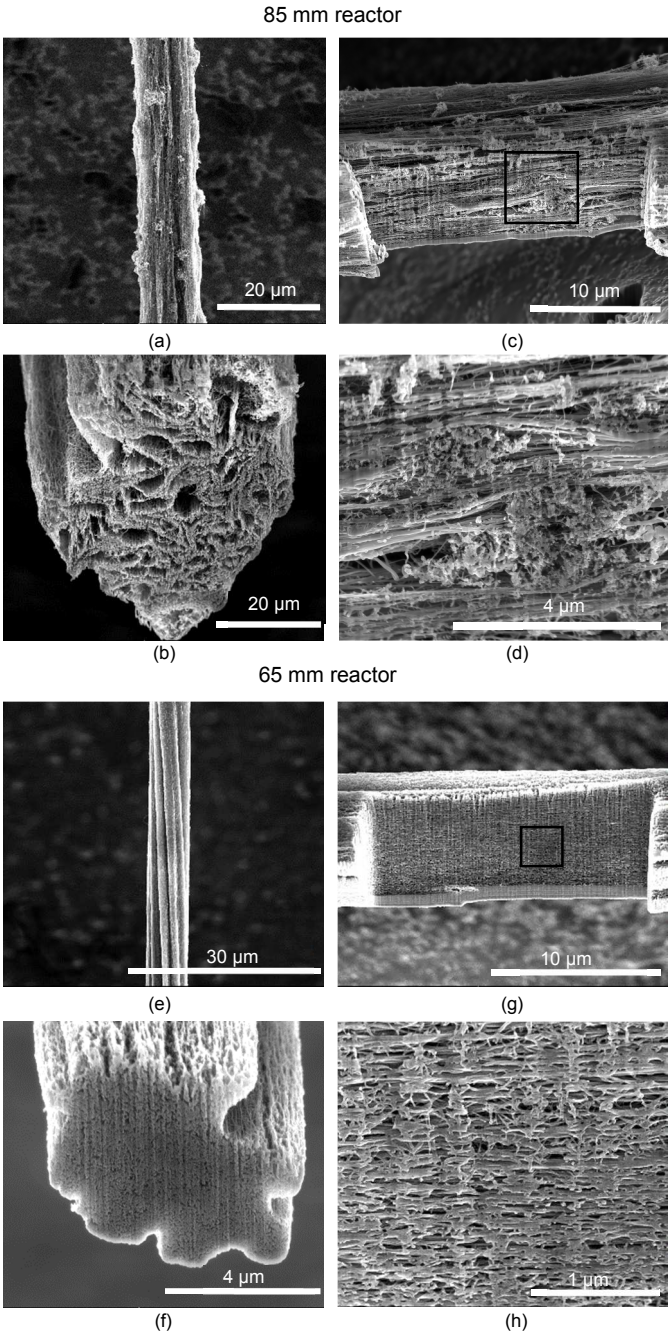


*Figure 4: SEM pictures of (a) the 'standard condition' impure fibre showing the big cluster impurities at the outside. FIB milled cross (b) and longitudinal (c, d) sections show the significant internal voids as the nanotubes 'flow' around the impurity particles. (e) The fibres spun with a steeper velocity profile resulting from the smaller diameter reactor tube show a much cleaner structure with no cluster impurities. The cross- (f) and longitudinal (g, h) sections show the highly improved density and uniformity of the cleaner fibre.*

In contrast, the material from the smaller diameter reactor shows only one main combustion event around 650°C (Figure 5b) which is in the range of the 'clean bundles peak' of the impure fibre, although slightly shifted to lower temperatures. Additionally, the iron residue, for the same rate of iron input, is dramatically reduced to only 1.5% compared with > 15% before. This order of magnitude decrease reflects the absence of the large Fe particles causing the impurity clusters.

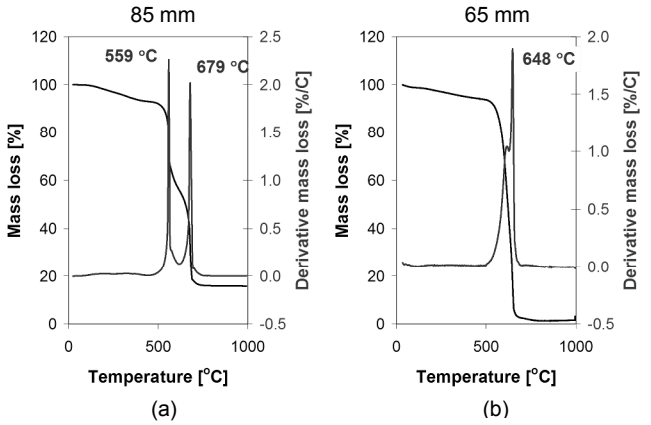


*Figure 5: Thermogravimetric analysis of (a) impure fibre material and (b) clean CNT fibre material, spun with a steeper velocity profile. In the impure material the carbon impurity clusters burn first, due to the highly defective structure and catalysed by intern.*

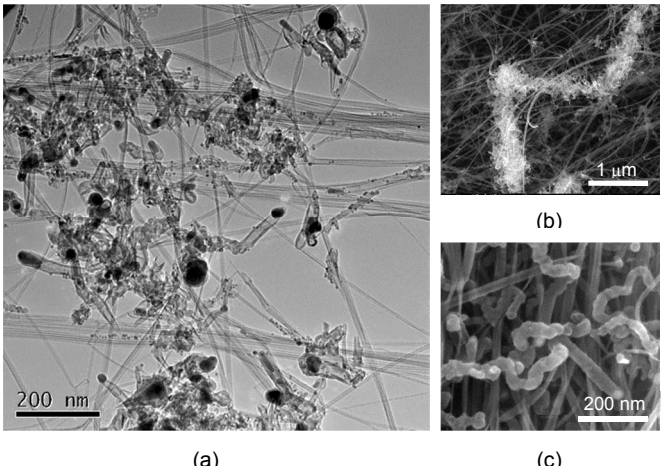


*Figure 6: (a) TEM of poorly formed MWCNTs grown from big Fe particles clustered together in standard material, (b) SEM of chained clusters in uncondensed standard material of several micrometres in length, (c) SEM of occasionally observed deformed but un-clustered tubular structures in clean fibre.*

In order to understand why the faster flow means greater purity, we need to consider how these clusters associated with larger iron particles come to be incorporated. We propose that it is the poorly formed multiwall CNTs which grow from their surfaces which provide the necessary opportunity for them to become entangled with the main aerogel and thus pulled from the reactor with the fibre and incorporated into it on condensation. We have observed these larger clusters forming chains on the surface of the fibre (Figure 6).

For the faster flow in the 65 mm reactor tube the average residence time of the particles in the reaction zone is decreased by 70% (SOM4), which would appear to provide insufficient opportunity for slow moving, larger iron particles to grow their own nanotubes to a length sufficient for them to entangle both with their large neighbours and the main aerogel. In the 'clean' fibre we still observe (Figure 6c, SOM1), albeit very occasionally, poorly formed nanotubes growing from larger particles, but the nanotubes there are much shorter, and do not appear to form clusters.

**The critical role of sulphur**

The process is dependent on the addition of sulphur, the role of which in high temperature floating catalyst CNT synthesis has been variously ascribed to:

a. Acting as a promoter to enhance the addition of carbon atoms to the growing ends of the graphene tubes. [24]
b. Acting as a surfactant to encourage tube nucleation and thus prevent carbon encapsulation of the catalyst particle. Sulphur is also understood as a surfactant in affecting the growth of graphitic phase during the solidification of cast irons [25, SOM5]
c. Limiting the rate at which the iron particles coarsen by collision. [15]

One major challenge in studying the process to make CNT fibre is that one is operating in multi-dimensional parameter space, and changing any one parameter beyond a limited 'window' while keeping all other parameters constant usually moves out of the continuous spinning window. The switch from methane to toluene as the carbon source, with the same rate of input of carbon, prevented the process from working, with much carbonaceous material being formed but no spinnable aerogel. We took the view that the greater availability of carbon from toluene as opposed to the much more stable methane, especially at lower temperatures, meant that there was oversupply. Indeed on reducing the nominal carbon input rate by a factor of 20, spinning was restored. Under these conditions it was found that the concentration of sulphur could be reduced by a factor as large as 42 while still maintaining stable spinning. The conditions are summarised in Table 2.

When starting the synthesis without any sulphur added, stable spinning could never be achieved. However, if spinning with thiophene (S:C = 0.02) and then terminating its injection, stable spinning continued for about 23 min whereupon it ceased and could not be re-established again. We consider that as sulphur will be present on the inside of the reactor vessel, it takes some time before the equipment is complete purged of that component. We also noted a very considerable carbon build up in the reactor while the rig was operating at zero sulphur. We conclude that continuous spinning of CNT fibres using this process is not possible without the addition of sulphur.

.

*Table 2: Spinning conditions with low sulphur and carbon in a reactor tube with inner diameter of 65 mm*

| | Flow rates | | | | Total atomic ratio | | Average linear density of fibre [tex] | Mass ratio of CNTs 'out' to total carbon 'in'. |
|---|---|---|---|---|---|---|---|---|
| | H2 [l/min] | Carbon precursor | Ferrocene [mg/min] | Thiophene [mg/min] | S:C | S:Fe | | |
| Standard chemistry, steeper velocity profile sample | 0.8 | Methane 80 ml/min | 0.35 | 1.3 | 0.004 | 7.65 | 0.02 | 0.015 |
| Early carbon (toluene), low sulphur sample | 1.1 | Toluene 1.37 mg/min | 1.0 | 0.03 | 0.002 | 0.06 | 0.035 | 0.35 |

**Structural characterization of low-sulphur CNT fibres.** The fibres were as clean as those generated using methane in the 65 mm reactor tubes. Figure 7b and c show a surface view of uncondensed material and a FIB section through a condensed fibre. Along with [31,32] we observed that as the amount of sulphur was reduced the mean number of walls in the nanotubes decreased, so that at the low sulphur limit, the nanotubes were predominately single wall.

Figure 7a shows the single wall nanotubes resolved in the TEM, while Figure 8a shows the Raman spectra which reveal strong Radial Breathing Mode (RBM) peaks which are a finger print of single wall nanotubes. Figure 8b is the equivalent Raman spectrum of the standard conditions fibre discussed above. The D/G ratio indicating the proportion of badly formed (or edge related) carbon is much reduced for the low sulphur, single wall sample. The RBMs appear mainly at two wavenumbers, 161 and 252 cm-1, indicating according to $\omega_{RBM} = (223.5\ cm^{-1} \cdot nm / d_{CNT}) + 12.5\ cm^{-1}$ [33], CNTs of 0.9 to 1.5 nm diameter, which is compatible with the measurements from TEM. Our model for the critical role played by sulphur in direct spinning of CNT fibre draws also from the wider catalysis literature.

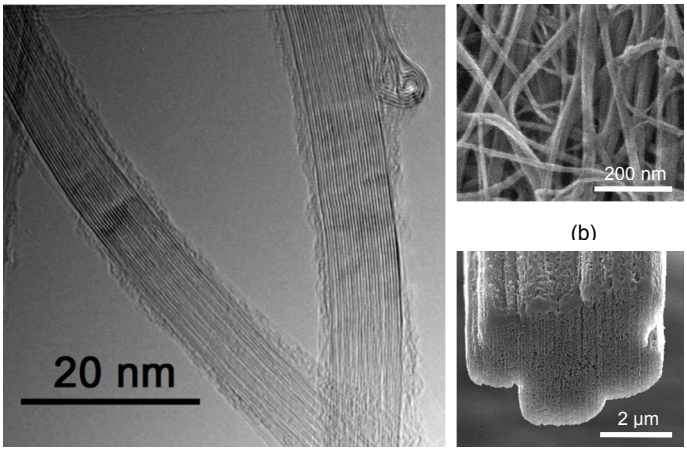


*Figure 7: (a) TEM image of SWCNT bundles, (b) SEM image of a toluene fibre with CNT bundle diameters of 8 – 27 nm, and (c) the cross section of a condensed fibre cut by focussed ion beam. The outside of the FIB milled fibre looks slightly molten as carbon re-deposits on the surface whilst the cross section is cut by the ion beam.*

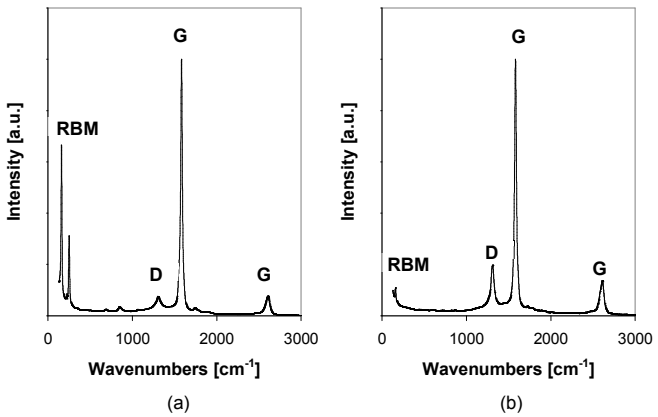


*Figure 8: (a) Raman spectra of Toluene fibre showing the typical, very distinct RBM peaks, which correspond to CNTs with diameters of 0.9 and 1.5 nm and a very low D/G ratio of 0.05. (b) Raman spectra of standard material showing a D/G ratio of 0.19; infrequently, RBMs can be observed even in the standard material indicating the occasional SWCNTs, usually however there are no RBMs to be observed.*

**A model for the role of sulphur.** Sulphur features largely in the literature associated with the catalysis of organic reactions by metal, particularly transition metal, particles. Sulphur has been known as a catalyst poison where even trace amounts of the element in hydrocarbon feedstock can drastically reduce the activity of a catalyst, [34,35]. However, somewhat more recently it has become clear that distinctly beneficial effects can follow from the partial and well controlled poisoning of metals by sulphur [25,36]. This opens up the possibility that control of sulphur to provide only partial coverage of the iron catalyst particles in the CNT floating catalyst process may provide distinct benefits.

It is now well established that the diameter of the carbon nanotube is closely related to the diameter of the catalyst particle generating it, at least in the smaller diameter range. In the case of synthesis from methane, not only will the sulphur be available before carbon, but with 8 sulphur atoms available per iron atom (standard conditions), for the case of a 1nm iron particle where approximately two thirds of the iron atoms are surface atoms, the conditions would appear to be ripe for total sulphur poisoning of the catalyst. Setting aside for the moment that fibres were nevertheless produced under these conditions, if we consider the other extreme, that of no sulphur, then we are unable to make nanotubes of sufficient quality and quantity to make fibre. Carbon products are generated and some nanotubes too,

however TEM examinations shows a profusion of catalyst particles 'blinded' by a continuous carbon coating (Figure 9).

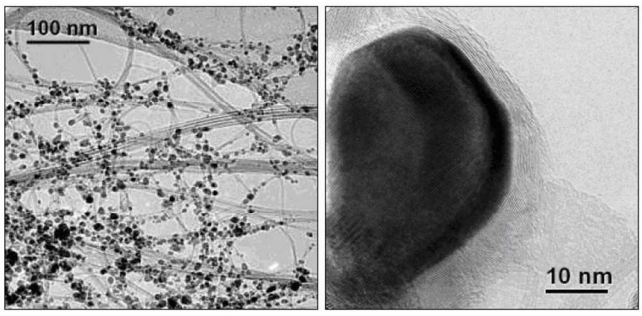


*Figure 9: TEM micrographs of the carbonaceous material generated in the reactor under conditions of zero sulphur where it was impossible to spin fibres. Although there are some nanotubes, the material is dominated by catalyst particles completely encased in graphene layers. (Courtesy Prof. I. A. Kinloch)*

The S:Fe ratio, 0.06, at which we obtained single wall CNT fibre, with a high carbon conversion efficiency, would mean the partial covering (~12%) for iron particles 1 nm in diameter. These conditions would avoid poisoning and yet mean that sulphur is available in its surfactant role for the early available carbon whether from thiophene, ferrocene or toluene. However, the fact that we were not successful in spinning with low sulphur using methane instead of toluene would imply that it is the combination of critical sulphur delivery and comparatively early carbon availability which is key to the generation of nanotube nucleation before the iron particles have grown by collision. The process is illustrated in Figure 10a.

A previous report from this laboratory demonstrated the spinning of single wall CNT fibres using carbon disulphide as the sulphur source [15]. Here, the amount of sulphur added was larger than in this case. However, we note that the catalysed thermolysis of carbon disulphide would liberate available carbon at the same time as sulphur, and thus the key condition of having iron particles partially coated with sulphur may still be met. The single wall CNTs in the fibres generated in this experiment were also predominately 'arm chair' and thus metallic in nature. The single wall material generated here, although showing two or perhaps three predominant RBM peaks in the Raman (Figure 8a), are not singularly of one chirality. The reason for 'armchair' dominance in the previous case is the subject of on-going studies.

We now need to return to the question as to why, if the recently nucleated iron particles are completed coated and 'blinded' by sulphur, which will occur when the sulphur is available in significant quantities before carbon, as for 'standard conditions', we are successful in growing nanotubes at all, given that they are now of significantly larger diameter with only occasional single wall examples detected.

An indication of the answer to this question comes from a consideration of the thermodynamic stability of iron sulphide (FeS). The free energy 'Ellingham' diagram (SOM5) can be read to show that for standard conditions, where the maximum possible value of $H_2S/H_2$ is $4 \cdot 10^{-4}$, hydrogen would extract sulphur from FeS above 1150°C to form $H_2S$. This temperature depends on the ratio of sulphur to hydrogen injected into the reactor. For higher sulphur/hydrogen ratios the temperature would increase and vice versa. However, as the sulphur is surface adsorbed rather than incorporated within the crystal structure, these temperatures must be regarded as a first estimate.

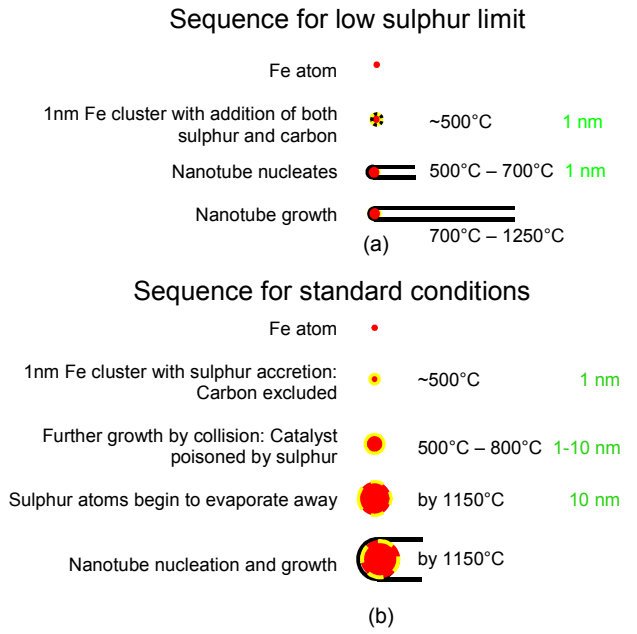


*Figure 10: (a) For low sulphur conditions, the 1 nm Fe clusters (estimated particle diameters in green) experience a balanced arrival of both sulphur and carbon. The nanotubes nucleate, with sulphur preventing carbon encapsulation. Further iron growth by collision is thought to be prevented by the nanotube nucleus. (b) For standard conditions, from the point of availability of sulphur, the sulphur accretes on the 1 nm Fe cluster. Further particle growth by collision can occur despite the sulphur on the surface, the catalytic property is however hemmed by sulphur poisoning. At temperatures above 1000°C, the sulphur atoms begin to evaporate away, hence, carbon atoms have access to Fe and nucleate a CNT.*

The possibility of sulphur being lost from a catalyst particle at higher temperatures than that at which it was deposited was also pointed out in a paper from before the CNT era [25]. We thus propose that the larger diameter, multiwall nanotubes which comprise the fibres spun under high sulphur regimes, occur because the growing iron particles, initially poisoned by sulphur, become active, after further growth by collision, when the sulphur begins to be lost to $H_2S$ as the reactants move into the higher temperature regions of the reactor. At this point the active particles are in the presence of available hydrogen, the two conditions for nanotube growth.

The issue of whether sulphur will lower, or even prevent, the coarsening of the iron particles by collision was discussed in [15]. While the current observations suggest that coarsening is not prevented completely, it is very possible that sulphur coated particles may not coarsen as rapidly as uncoated ones, simply on the basis that the primary sulphur bonds are satisfied by their contact with iron, so that a sulphur coated particle may be less 'sticky' in bonding terms.

The model for the growth of multiwall nanotubes from the floating catalyst process, involving first complete poisoning by sulphur followed by its partial loss in the presence of available carbon, is shown in Figure 10b.

### Mechanical properties

So far this study has related processing conditions to both purity and the structure of the carbon nanotubes comprising the fibres. However, one major potential application of the CNT fibre will stem from its unique spectrum of mechanical properties. The experiments described above, based on enhanced control of the process, have provided samples which provide new data on the influence of both purity of fibre and diameter of nanotubes on mechanical strength.
Stress strain curves comparing standard conditions fibre (impure), fibre based on similar nanotube structure but with greatly reduced particulate impurities, and fibre also with low particulate impurities but comprising almost entirely of single wall nanotubes are compared in Figure 11.

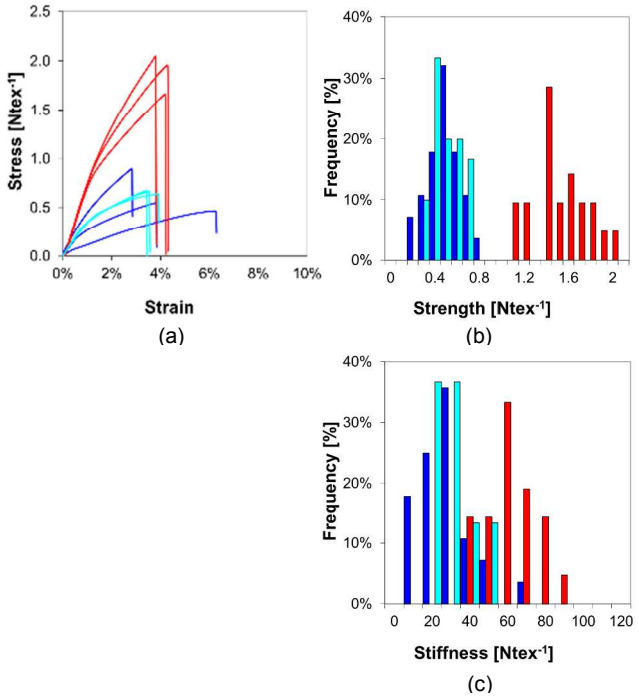


*Figure 11: (a) Selected typical stress-strain curves at 20 mm gauge length are shown for standard conditions (sample 1, dark blue), standard chemistry, but cleaner fibre (sample 2, turquoise), and SWCNT fibre (sample 3, red). (b) and (c) show the average strength and stiffness of 25 tests each. Low sulphur – toluene fibre compared to the standard fibre showed strength and stiffness increased by a factor of 2.8 and 2.5, respectively.*

Figure 11b and c compare the strength and stiffness of the three fibre classes, in each case the values being the averages of 25 stress strain curves. The tests were carried out on samples of gauge length approximately 2000 times the fibre diameter, using a Favimat dedicated fibre tester, in which the linear density of each tensile specimen was measured by detecting the natural vibration frequency. Comparing first the standard conditions fibre and the much purer derivative (dark blue and turquoise in Figure 11), it is interesting that the much cleaner fibre is no stronger than the one full of particles. The reasonable expectation, based on virtually all other high strength fibres, that the elimination of second phase (particulate) impurities would increase the strength does not apply in this case. The fact that the aligned yet flexible nanotube bundles 'flow' around impurity particles, rather as wood grain does around knots, gives a rationale as to why the particles do not initiate fracture at lower stresses. Interestingly though, there is a marked increase in the initial stiffness on purification. The reason for this is illustrated in Figure 12. The condensation process produces a structure which wraps around the particle, but is capable of extension on stressing thus reducing the initial elastic modulus. The standard deviation in the values of stiffness was decreased from 46% for to 14% by the elimination of particulate impurities.

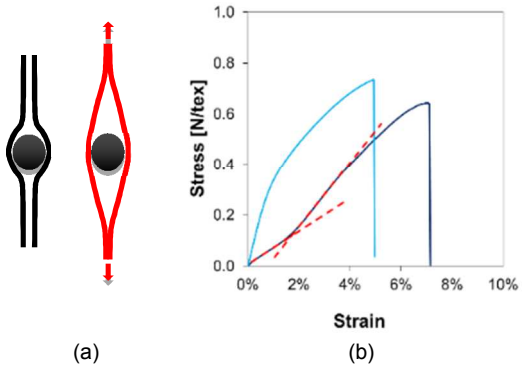


*Figure 12: (a) In a tensile test of fibres containing impurities the stretching of the bundles bent by the impurities can cause an initial region with a less steep slope (dark blue in (b)). Clean fibres (turquoise) are already optimally condensed and aligned, therefore leading to a higher slope of the tensile curve.*

The samples produced under conditions of sulphur control which produce single wall nanotubes show markedly different mechanical properties, as apparent from Figure 11 (red curves). Although the microstructure of the fibre, as observed by SEM, is virtually indistinguishable from the purified version of the standard fibre, the strength is nearly trebled with values approaching 2 $Ntex^{-1}$. Furthermore, the stiffness is increased by approximately a factor of two. While this result is encouraging in terms of the applicability of the fibre, we do not yet definitely understand the origin of the increased properties. They do not seem to be related to the level of particulate impurities, so we must assume that they are associated with the more efficient sharing of stress in bundles of single wall CNTs compared with the case of larger diameter multiwall tubes, some of which are collapsed.

## Conclusions

One of the key aspects of the continuous process to spin carbon nanotube fibres directly from the nanotube synthesis zone is the fact that the nanotubes, as they are synthesised, only qualify for removal as a fibre once they are long enough to entangle and create an aerogel. This 'mechanical fractionation' of the synthesised material should, ideally, ensure that the fibres are entirely of long nanotubes. In general, this condition has not been met. The origin of impurities based on larger catalyst particles growing poorly formed multiwall nanotubes has been identified, firstly with the slow moving component of the Poiseuille flow near to the reactor walls, and then with the engagement of the 'hairy clusters' with the main aerogel (and indeed sometimes with each other), and their resultant removal as unwanted components of the fibre. An increase in gas stream

mean velocity for identical injection rates and proportions, has been achieved through the device of reducing reactor tube diameter. It has been demonstrated that the poorly formed clusters are no longer incorporated in the fibre, presumably because their occasionally occurring defective nanotube overgrowths are not sufficiently developed to cause this problem. The reduction in particle count is dramatic, while the amount of residual iron as determined by TGA and the proportion of graphitic material which is defective in terms of a high D/G ratio on the Raman spectrum is also marked. Interestingly though, the very considerable increase in perfection does not lead to a concomitant improvement in fibre strength, although both the stiffness and the variability in this parameter from sample to sample is definitely increased.

It has proved possible to spin fibres consisting almost entirely of single wall CNTs limiting sulphur addition to a critically controlled low level, and also supplying carbon as a precursor (in this case toluene) which has a lower pyrolysis temperature than methane. Again the fibres do not contain extraneous particulate clusters, and the residual iron content is low. We determined also that it is impossible to spin fibre in the complete absence of sulphur, although it is important to completely purge the reactor from residual sulphur otherwise one might be initially misled. The fact that nanotubes could be nucleated from iron particles before they had grown to beyond 1 nm diameter by collision is explained in terms of the precepts of the catalyst science, where partial coating of metal catalyst by sulphur enhances activity while complete coverage effectively passivates the particle, as indeed does complete encapsulation by a graphene shell (at least in the case of floating catalysts). This model, however, needs to be applicable to standard conditions fibres. Here we propose a model based on the premise that where sulphur is added in larger amounts the metal particles are initially fully passivated by sulphur, while continuing to grow by collision (albeit possibly at reduced rate). However, as the reactants move into the higher temperature zone of the reactor, the sulphur is predicted to be lost as $H_2S$, exposing at a critical juncture partially sulphur covered iron particles to available carbon, again achieving the conditions for nanotube nucleation and growth. The mechanical properties of the single wall CNT fibres are greatly improved compared with the multiwall 'standard' material, with the mean strength of the samples increased by nearly a factor of 3. The exact reasons for this marked and extremely useful enhancement are still being explored.

## Acknowledgements

The authors wish to thank the *U.S. Office of Naval Research Global*, and *Innovative Material Synergies and Composite Processing Strategies* for funding.

## Notes and references

[a] Department of Materials Science and Metallurgy, University of Cambridge.

Electronic Supplementary Information (ESI) available: [details of any supplementary information available should be included here]. See DOI: 10.1039/b000000x/

1 Y.-L. Li, I. A. Kinloch, and A. H. Windle, *Science* 2004, **304**, 276;
2 Marcelo Motta, Ya-Li Li, Ian Kinloch, and Alan Windle, *Nano Lett.*, 2005, **5**, 1529;
3 K. Koziol, J. Vilatela, A. Moisala, M. Motta, P. Cunniff, M. Sennett, and A. Windle, *Science,* 2007*,* **318**, 1892;
4 J. J. Vilatela, and A. H. Windle, *Adv. Mater*., 2010, **22**, 4959;
5 B.G. Demczyk, Y.M. Wang, J. Cumings, M. Hetman, W. Han, A. Zettl,, and R.O. Ritchie, *Mater. Sci.Eng.,* 2002, **A334**, 173;
6 M.-F. Yu, O. Lourie, M. J. Dyer, K. Moloni, T. F. Kelly, and R. S. Ruoff, *Science*, 2000, **287**, 637
7 Marcelo Motta, Anna Moisala, Ian A. Kinloch, and Alan H. Windle, *Adv. Mater.* 2007, **19**, 3721;
8 A. B. Dalton, S. Collins, J. Razal, E. Munoz, V. H. Ebron, B. G. Kim, J. N. Coleman, J. P. Ferraris, and R. H. Baughman, *J. Mater. Chem.,* 2004, **14**,1;
9 N. Behabtu, C. C. Young, D. E. Tsentalovich, O. Kleinerman, X. Wang, A. W. K. Ma, E. A. Bengio, R. F. Waarbeek, J. J. de Jong, R. E. Hoogerwerf, S. B. Fairchild, J. B. Ferguson, B. Maruyama, J. Kono, Y. Talmon, Y. Cohen, M. J. Otto, and M. Pasquali, *Science,* 2013, **339**, 182;
10 M. Zhang, K. R. Atkinson, and R. H. Baughman, *Science*, 2004, **306**, 1358;
11 M. D. Lima, S. Fang, X. Lepró, C. Lewis, R. Ovalle-Robles, J. Carretero-González, E. Castillo-Martínez, M. E. Kozlov, J. Oh, N. Rawat, C. S. Haines, M. H. Haque, V. Aare, S. Stoughton, A. A. Zakhidov, and R. H. Baughman, *Science*, 2011, **331**, 51;
12 H. G. Chae, and S. Kumar, *Science*, 2008, **319**, 908;
13 D. Conroy, A. Moisala, S. Cardoso, A. Windle, and J. Davidson, *Science,* 2010, **65**, 2965;
14 K. Kuwana, and K. Saito, *Carbon*, 2005, **43**, 2088;
15 R. M. Sundaram , K. K. Koziol, and A. H. Windle, *Adv. Mater.*, 2011, **23**, 5064;
16 (a) G. Segre, and A. Silberberg, *Nature*, 1961, **189**, 209; (b) G. Segre, and A. Silberberg, *J. Fluid Mech.*, 1962, **14**, 136;
17 R. V. Repetti, and E. F. Leonard, *Nature,* 1964*,* **203**, 1346;
18 A. Barreiro, S. Hampel, M. H. Ru1mmeli, C. Kramberger, A. Grüneis, K. Biedermann, A. Leonhardt, T. Gemming, B. Bu1chner, A. Bachtold, and T. Pichler, *J. Phys. Chem. B*, 2006, **110**, 20973;
19 K. Elhin, Dissertation "Synthesis of carbon-covered iron nanoparticles by photolysis of ferrocene", University Upsala 2002;
20 L. M. Dyagileva, V. P. Mar'in, E. I. Tsyganova, and G. A. Razuvaev, *J. Organomet. Chem.*, 1979, **175**, 63
21 S. G. Gagarin, Yu. A. Teterin, and Yu. V. Plekhanov, *Theoretical and Experimental Chemistry*, 1989, **25**, 335
22 F. Zaera, E. B. Kollin, and J. L. Gland, *Surf. Sci.*, 1987, **184**, 75
23 M. Zonnevylle, R. Hoffmann, and S. Harris, *Surf. Sci.*, 1988, **199**, 320
24 G. G. Tibbetts, C. A. Bernardo, D. W. Gorkiewicz, and R. L. Alig, *Carbon*, 1994, **32**, 569;
25 M. S. Kim, N. M. Rodriguez, and R.T.K. Baker, *J. Catalysis*, 1993, **143**, 449;
26 M. A. Ermakova, D. Y. Ermakov, A. L. Chuvilin, and G. G. Kuvshinov, *J. Catalysis*, 2001, **201**, 183;
27 T. V. Reshetenko, L. B. Avdeeva, Z. R. Ismagilov, V. A. Ushakov, A. L. Chuvilin, and Y. T. Pavlukhin, *Chem. Sust. Dev.*, 2003, **11**, 239;
28 A. Konieczny, K. Mondal, T. Wiltowski, and P. Dydo, *Internat. J. Hydrogen Energy,* 2008, **33**, 264;
29 X. Ma, A. A. Lall, N. Aronhime, and M. R. Zachariah, *Internat. J. Hydrogen Energy*, 2010, **35**, 7476;
30 M. Motta, and A. Moisala - unpublished report, 2008
31 W. Ren, F. Li, S. Bai, and H.-M. Cheng, *J. of Nanosci. Nanotech.,* 2006, **6**, 1339;
32 V. Regero, B. Alemán, B. Mas, and J. J. Vilatela, *Chem. Mater.,* 2014*, submitted*

33 S. M. Bachilo, M. S. Strano, C. Kittrell, R. H. Hauge, R. E. Smalley, and R. B. Weisman, *Science*, 2002, **298**, 2361;
34 R. A. Dalla Betta, A. G. Piken, and M.J. Shelef, *J. Catalysis*, 1975, **40**, 173;
35 J. Oudar, *Catal. Rev. Sci. Eng.* 1980, **22**, 171;
36 C.H. Bartholomew, G. D. Weatherbee, and G. A. Jarvi, *J. Catalysis*, 1982, **60**, 257;



 